Paper AAS 03-579

Interplanetary Mission Analysis for Non-Perfectly Reflecting Solar Sailcraft Using Evolutionary Neurocontrol

Bernd Dachwald
German Aerospace Center (DLR), Cologne

AAS/AIAA Astrodynamics Specialist Conference

Big Sky Resort, Big Sky, Montana, August 3-7, 2003

AAS Publications Office, P.O. Box 28130, San Diego, CA 92198

AAS/AIAA Astrodynamics Specialist Conference 2004, Big Sky, Montana, 03-07 August 2003

AAS 03-579

INTERPLANETARY MISSION ANALYSIS FOR NON-PERFECTLY REFLECTING SOLAR SAILCRAFT USING EVOLUTIONARY NEUROCONTROL

Bernd Dachwald*

Solar sailcraft trajectories are typically presented for high-performance sailcraft, assuming that the sail is an ideal reflector, or considering the non-ideal reflectivity through an overall efficiency factor. Otherwise, using traditional local trajectory optimization methods, it is difficult to generate the required initial guess. A real solar sail, however, is not a perfect reflector and a thorough trajectory simulation must therefore take into account the optical characteristics of the real sail film that lead not only to a reduced magnitude of the solar radiation pressure force but also to a directional deviation.

Within this paper, minimal transfer times for rendezvous missions within the inner solar system are presented for perfectly and non-perfectly reflecting solar sailcraft, including a typical near-Earth asteroid rendezvous ($1996FG_3$) and a typical main belt asteroid rendezvous (Vesta). For the different solar radiation pressure force models, the minimal transfer times are compared, extending thereby the currently available data to moderate-performance sailcraft of the first generation.

Using evolutionary neurocontrol as a global trajectory optimization method, it is shown that there is a considerable increase of about $5 - 15\%$ in the minimal transfer times, if the non-perfect reflectivity of the solar sail is taken into account. This fact must be considered for a thorough mission analysis. The simplification that the non-ideal reflectivity of the sail can be modelled with an overall sail efficiency factor should only be made for very preliminary mission analyses.

INTRODUCTION

Utilizing solely the freely available solar radiation pressure (SRP) for propulsion, solar sails provide a wide range of opportunities for innovative low-cost high-energy missions, many of which are difficult or even impossible using any other type of conventional propulsion system.

Employing traditional **local trajectory optimization methods** (LTOMs) that are based on optimal control theory, it is – as for *all* low-thrust spacecraft – usually a difficult and lengthy task to find time-optimal solar sailcraft trajectories. A lot of experience and expert knowledge is required to conceive an adequate initial guess that is needed prior to optimization. Even if the optimizer converges to an "optimal solution", this solution is typically a local optimum that is close to the initial guess, which is rarely close to the global optimum.

* Research Engineer. German Aerospace Center (DLR), Cologne, Institute of Space Simulation, Space Missions and Technologies Section, Linder Hoehe, 51147 Koeln. E-Mail: bernd.dachwald@dlr.de Phone: +49-2203-601 3001 Fax: +49-2203-601 4655

Up to now, solar sailcraft trajectories have been typically presented for high-performance sailcraft, assuming that the solar sail is an ideal reflector or considering the non-ideal reflectivity through an overall efficiency factor that reduces only the magnitude of the SRP force but leaves its direction unaltered (Refs. [1, 2, 3, 4, 5]). In both cases, the direction of the SRP force is *always* perpendicular to the sail surface, so that both SRP force models can be considered as models of perfect (i.e. specular) reflection. The simplification of perfect reflectivity as well as the limitation on high-performance sailcraft seems to be mainly caused by the difficulty to generate adequate initial guesses for LTOMs.[†]

Nevertheless,

1. taking the current state-of-the-art in engineering of ultra-lightweight structures into account, solar sailcraft of the first generation will be of relatively moderate performance, and,
2. as it will be shown in this paper, a thorough mission analysis must consider the optical properties of the real non-perfectly reflecting sail film, where the SRP force has also a component parallel to the sail surface.

It is demonstrated in Refs. [7, 8, 9] that artificial neural networks in combination with evolutionary algorithms can be applied as **evolutionary neurocontrollers** for optimal solar sailcraft steering, and that they are often able to find better trajectories that are closer to the global optimum, since they explore the trajectory search space more exhaustively than a human expert, using LTOMs, can do. Using evolutionary neurocontrol as a smart **global trajectory optimization method** (GTOM), near-globally optimal trajectories can also be calculated for non-perfectly reflecting solar sailcraft of moderate performance.

SOLAR RADIATION PRESSURE FORCE MODELS

For the optical characteristics of a solar sail, different assumptions can be made, which result in different models for the magnitude and direction of the SRP force acting on the sail. The most simple model assumes an ideally reflecting sail surface. It will here be denoted as model IR (**Ideal Reflection**). With the intention to model the non-ideal reflectivity of a real solar sail, an overall **sail efficiency factor** η is typically used in the solar sail-related literature that reduces only the magnitude of the SRP force but leaves its direction unaltered. This model will here be denoted as model ηPR (η**-Perfect Reflection**). Since a real solar sail is *not* a perfect reflector, a thorough trajectory simulation must employ a more sophisticated SRP force model, which takes into account the optical characteristics of the real sail film. This model will here be denoted as model NPR (**Non-Perfect Reflection**). Table 1 gives an overview of the properties of the three SRP force models that are considered within this paper.

IR	(Ideal Reflection)	ideal reflection	perfect reflection
ηPR	(η-Perfect Reflection)	non-ideal reflection	perfect reflection
NPR	(Non-Perfect Reflection)	non-ideal reflection	non-perfect reflection

Table 1 SRP force models considered within this paper

All three SRP force models do not take into account the shape of the sail film under load but assume a plane sail surface. During the study for a comet Halley rendezvous mission with a solar sail, which has been performed at NASA/JPL in 1976–77, also a numerical parametric force model

[†] Trajectories for moderate-performance sailcraft involve typically multiple revolutions about the Sun. For non-perfectly reflecting solar sails, the locally optimal sail attitude can not be derived analytically from the locally optimal thrust direction, as it might be obtained from local steering laws (like LAGRANGE's planetary equations, Ref. [6] pp. 484–490).

has been developed, which considers the exact shape of the sail under load (Ref. [10]). Recently, also numerical analyses to predict the effects of structural wrinkles in the stressed sail film have been performed (Ref. [11]). Since those models, however, depend essentially on the actual sail *design*, they are not used within this paper.

For expressing the SRP force exerted on a solar sail, it is convenient to introduce two unit vectors. The first one is the **sail normal vector n**, which is perpendicular to the sail surface and always directed away from the Sun. Its direction, which describes the sail attitude, is – according to Figure 1.1 – usually expressed by the **sail clock angle** α and the **sail cone angle** β. The second unit vector is the **thrust unit vector f**, which points always along the direction of the SRP force. Its direction is described likewise by the **thrust clock angle** γ and the **thrust cone angle** δ – according to Figure 1.2.

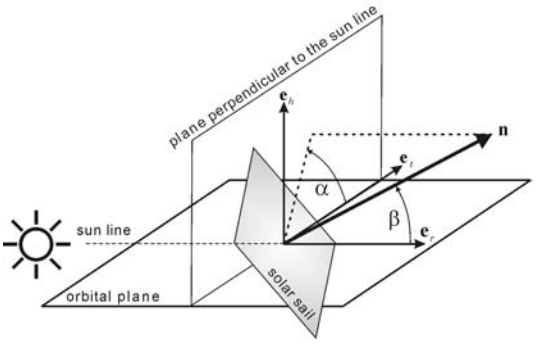

1.1: Definition of the sail clock angle α and the sail cone angle β

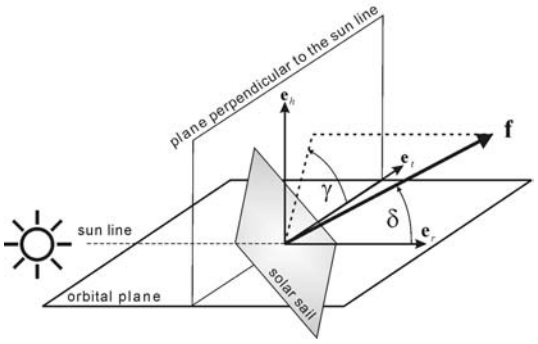

1.2: Definition of the thrust clock angle γ and the thrust cone angle δ

Figure 1 Definition of the sail normal vector (1.1) and the thrust unit vector (1.2)

The **solar radiation pressure** (SRP) at a distance r from the Sun is

$$P = \frac{S_0}{c}\left(\frac{1\,\mathrm{AU}}{r}\right)^2 \doteq 4.563\,\frac{\mu\mathrm{N}}{\mathrm{m}^2}\cdot\left(\frac{1\,\mathrm{AU}}{r}\right)^2 \tag{1}$$

where $S_0 = 1368\,\mathrm{W/m^2}$ is the well-known **solar constant** and c is the speed of light in vacuum.

SRP Force Models for Perfect Reflection (models IR and ηPR)

The force exerted on an ideally reflecting solar sail (model IR) can easily be calculated from Figure 2 (see also Ref. [10]). Using $\mathbf{e}_r$ and $\mathbf{e}_{r'}$ as the unit vectors along the direction of the incident and the reflected radiation, the force exerted on the sail due to the incident photons is $\mathbf{F}_r = PA(\mathbf{e}_r\cdot\mathbf{n})\mathbf{e}_r$, where $A(\mathbf{e}_r\cdot\mathbf{n})$ is the projected sail area along the $\mathbf{e}_r$-direction. The force exerted on the sail due to the reflected photons is $\mathbf{F}_{r'} = -PA(\mathbf{e}_r\cdot\mathbf{n})\mathbf{e}_{r'}$. Therefore, making use of $\mathbf{e}_r - \mathbf{e}_{r'} = 2(\mathbf{e}_r\cdot\mathbf{n})\mathbf{n}$, the total SRP force exerted on the sail is $\mathbf{F}_{\mathrm{SRP}} = \mathbf{F}_r + \mathbf{F}_{r'} = 2PA(\mathbf{e}_r\cdot\mathbf{n})^2\mathbf{n}$, and, making use of $\mathbf{e}_r\cdot\mathbf{n} = \cos\beta$,

$$\mathbf{F}_{\mathrm{SRP}} = 2PA\cos^2\beta\,\mathbf{n} \tag{2}$$

Looking at Eq. (2), one can see that the SRP force exerted on an ideally reflecting solar sail is always along the direction of the sail normal vector, $\mathbf{f} = \mathbf{n}$.

In the solar sail-related literature, an SRP force model is typically employed that uses an overall sail efficiency factor η, which is intended to model the non-ideal reflectivity of the sail (model ηPR). Using this factor, the SRP force acting on the sail is described by

$$\mathbf{F}_{\mathrm{SRP}} = 2\eta PA\cos^2\beta\,\mathbf{n} \tag{3}$$

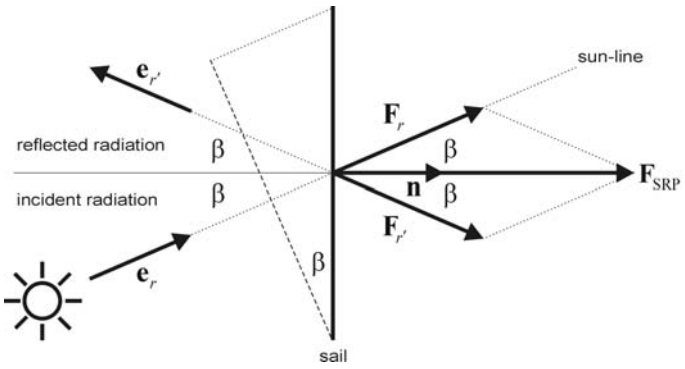

Figure 2 SRP force on a perfectly reflecting solar sail

Although model ηPR has no physical rationale and, as it will be seen, provides only a crude approximation of the real sail, it is widely used, because it allows an easy analytical treatment of solar sail mechanics (since also $\mathbf{f} = \mathbf{n}$).

SRP Force Model for Non-Perfect Reflection (model NPR)

Since a real solar sail is *not* a perfect reflector, a thorough trajectory simulation must consider the optical characteristics of the real sail film, which can be parameterized by the absorption coefficient α, the reflection coefficient ρ, the transmission coefficient τ, and the emission coefficient ε, with the constraint $\alpha+\rho+\tau = 1$. Assuming $\tau = 0$ for the reflecting side of the solar sail, the absorption coefficient is $\alpha = 1 - \rho$. Since for a real solar sail not all photons are reflected specularly, the reflection coefficient can be further divided into a coefficient for specular reflection ρ_s, a coefficient for diffuse reflection ρ_d, and a coefficient for back reflection ρ_b, with the constraint $\rho_s+\rho_d+\rho_b = \rho$. Assuming $\rho_b = 0$, this can also be expressed by introducing a specular reflection factor s, so that $s = \rho_s/\rho$ and thus $\rho_s = s\rho$ and $\rho_d = (1 - s)\rho$.

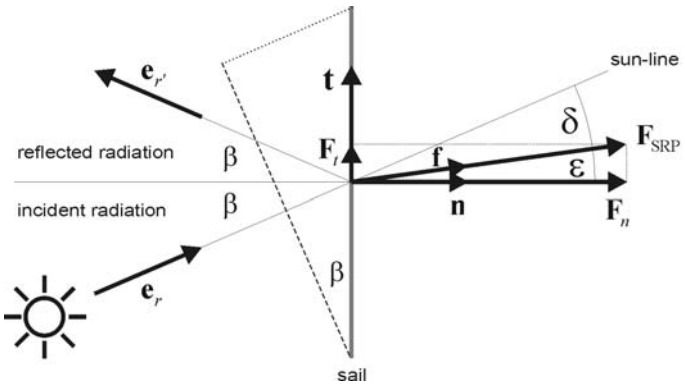

Figure 3 SRP force on a non-perfectly reflecting solar sail

It can be shown (see Ref. [10] for derivation) that, using those optical parameters, the SRP force exerted on the solar sail has a normal component $\mathbf{F}_n$ and a transversal component $\mathbf{F}_t$ (see Figure 3)

with

$$\mathbf{F}_n = PA\left((1+s\rho)\cos\beta + B_\mathrm{f}(1-s)\rho + (1-\rho)\frac{\varepsilon_\mathrm{f}B_\mathrm{f} - \varepsilon_\mathrm{b}B_\mathrm{b}}{\varepsilon_\mathrm{f}+\varepsilon_\mathrm{b}}\right)\cos\beta\,\mathbf{n} \tag{4a}$$

$$\mathbf{F}_t = PA(1-s\rho)\sin\beta\cos\beta\,\mathbf{t} \tag{4b}$$

where $\mathbf{t}$ is a transverse unit vector perpendicular to $\mathbf{n}$ (so that $\mathbf{t}\cdot\mathbf{e}_r \geq 0$), ε_f and ε_b are the emission coefficients of the sail's front and back side, and B_f and B_b are the non-LAMBERTian coefficients of the sail's front and back side. WRIGHT gives in Ref. [5] values for the optical coefficients for a sail with a highly reflective aluminum-coated front side and a highly emissive chromium-coated back side, to keep the sail temperature at a moderate limit (Table 2).

parameter	front side (Al-coated)	back side (Cr-coated)
ρ	0.88	
s	0.94	
ε	0.05	0.55
B	0.79	0.55

Table 2 Optical coefficients for an Al|Cr-coated solar sail

Using the values given in Table 2, three characteristic optical sail film coefficients may be defined to simplify Eqs. (4) (Ref. [12]):

$$G = 1 + s\rho = 1.8272 \tag{5a}$$

$$K = B_\mathrm{f}(1-s)\rho + (1-\rho)\frac{\varepsilon_\mathrm{f}B_\mathrm{f} - \varepsilon_\mathrm{b}B_\mathrm{b}}{\varepsilon_\mathrm{f}+\varepsilon_\mathrm{b}} = -0.010888 \tag{5b}$$

$$H = 1 - s\rho = 0.1728 \tag{5c}$$

so that

$$\mathbf{F}_n = PA\,(G\cos\beta + K)\cos\beta\,\mathbf{n} \tag{6a}$$

$$\mathbf{F}_t = PAH\sin\beta\cos\beta\,\mathbf{t} \tag{6b}$$

The total SRP force vector may then be written as

$$\mathbf{F}_\mathrm{SRP} = \sqrt{F_n^2 + F_t^2}\,\mathbf{f} = PA\sqrt{(G\cos\beta + K)^2 + H^2\sin^2\beta}\cos\beta\,\mathbf{f} \tag{7}$$

and, by defining $Q(\beta) = \frac{1}{2}\sqrt{(G\cos\beta + K)^2 + H^2\sin^2\beta}\cos\beta$

$$\mathbf{F}_\mathrm{SRP} = 2PAQ(\beta)\,\mathbf{f} \tag{8}$$

where $Q(\beta)$ depends only on the sail cone angle β and the optical coefficients of the sail film. The angle between $\mathbf{f}$ and $\mathbf{e}_r$ is the thrust cone angle δ and the angle between $\mathbf{f}$ and $\mathbf{n}$ is called **centerline angle** ϵ. It may be calculated via

$$\epsilon = \arctan\left(\frac{F_t}{F_n}\right) = \arctan\left(\frac{H\sin\beta}{G\cos\beta + K}\right) \tag{9}$$

Eq. (9) gives then also the relation for the thrust cone angle:

$$\delta = \beta - \epsilon = \beta - \arctan\left(\frac{H\sin\beta}{G\cos\beta + K}\right) \tag{10}$$

SRP Force Model Comparison

The orbital dynamics of solar sailcraft is in many respects similar to the orbital dynamics of other low-thrust spacecraft; however, as Figure 4 shows, other low-thrust spacecraft may orient its thrust vector into any desired direction, whereas the thrust vector of solar sailcraft is constrained to lie on the surface of a "bubble" that is always directed away from the Sun. Nevertheless, by controlling the sail orientation relative to the Sun, solar sailcraft can gain orbital angular momentum and spiral outwards – away from the Sun – or lose orbital angular momentum and spiral inwards – towards the Sun.

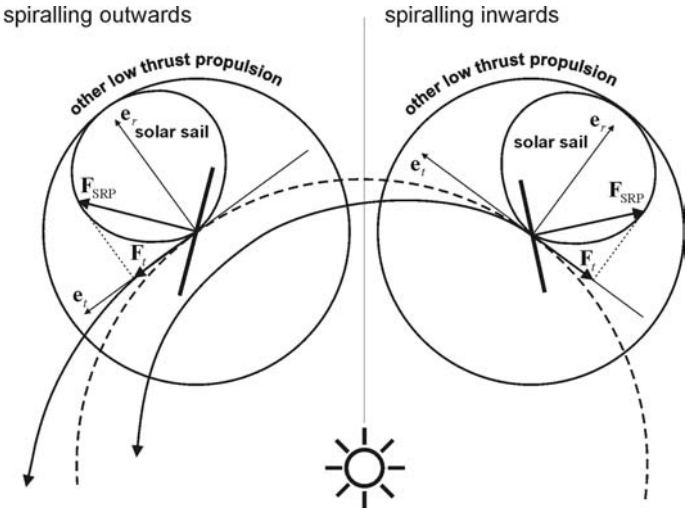

Figure 4 Spiralling towards the Sun and away from the Sun

For the models IR and ηPR, the SRP force is always perpendicular to the sail surface, $\mathbf{f} = \mathbf{n}$. This allows an easy analytical treatment of solar sail steering problems. If $\mathbf{d}$ denotes the unit vector along the desired thrust direction, the thrust unit vector $\mathbf{f}$ must point into the direction $\mathbf{f}^*$ that maximizes the SRP force along $\mathbf{d}$; $\mathbf{f}^*$ can be derived analytically from $\mathbf{d}$ (Ref. [9]):

$$\gamma^* = \arctan(d_h, d_t) \tag{11a}$$

$$\delta^* = \operatorname{arccot}\left(\frac{3}{2}\frac{d_r}{\sqrt{d_t^2 + d_h^2}} + \sqrt{\frac{9}{4}\frac{d_r^2}{d_t^2 + d_h^2} + 2}\right) \tag{11b}$$

where $\arctan(d_h, d_t)$ is an extended arcustangens, which gives the angle γ^* such that $d_h = \sin\gamma^*$ and $d_t = \cos\gamma^*$. The sail normal vector $\mathbf{n}$ – as expressed by the sail clock angle α and the sail cone angle β – is the **spacecraft control vector** $\mathbf{u} = (\alpha, \beta)$. The problem is to determine $\mathbf{u}$ so that $\mathbf{f} = \mathbf{f}^*$. For models IR and ηPR, $\mathbf{n}^* = \mathbf{f}^*$ and thus $\alpha^* = \gamma^*$ and $\beta^* = \delta^*$. For model NPR, $\mathbf{n}^*$ can *not* be calculated analytically from $\mathbf{f}^*$, since the $Q(\beta)$-expression can not be resolved for β. Hence, the spacecraft control vector that maximizes the SRP force along the desired thrust direction can not be obtained analytically.

Although the models IR and ηPR allow the analytical treatment of solar sail steering problems, they misrepresent the normal SRP force component $\mathbf{F}_n$ and completely ignore the transverse SRP force component $\mathbf{F}_t$. In doing so, both models ignore the deviation of the thrust cone angle from the sail cone angle. Figure 5.1 shows how this deviation becomes larger as the light incidence angle increases. As a consequence, the SRP force in model NPR is not only smaller than in model IR (which is also taken into account by model ηPR) but also much more constrained in its direction (Figure 5.1 shows that there is a maximum thrust cone angle of 55.5° for a sail cone angle of 72.6°).

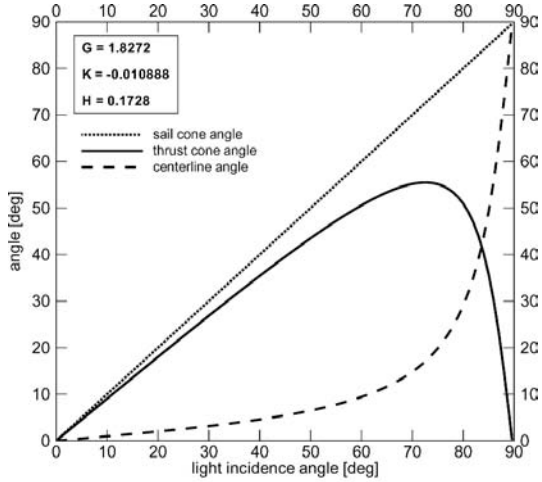

5.1: Angular deviations for the standard SRP force model (adapted from Ref. [10])

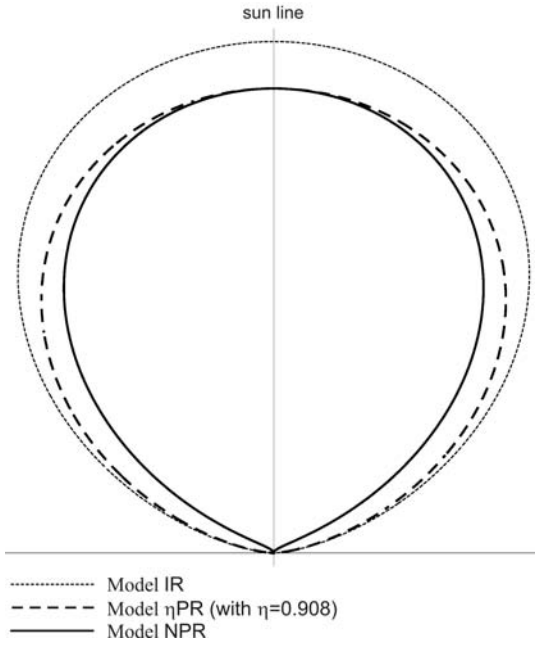

5.2: SRP force "bubbles" for the different SRP force models

Figure 5.2 shows for each SRP force model the "bubble" on whose surface the SRP force vector tip is constrained to lie (vector tail at origin). From the perspective of trajectory analysis, model ηPR is equivalent to model IR, since the *shape* of both bubbles is identical. A decrease in sail efficiency η can *always* be offset with a proportional increase in sail area, so that both bubbles have the same shape *and* size. This equivalency is not the case for model NPR. Even if the $\cos^2\beta$-bubble and the $Q(\beta)$-bubble are scaled to the same size, their shape is different.

SOLAR SAILCRAFT PERFORMANCE PARAMETERS

Eqs. (3) and (8) may also be expressed in terms of the **characteristic acceleration** a_c or in terms of the **lightness number** λ, which are the prevalent performance parameters for solar sailcraft.

Characteristic Acceleration

The characteristic acceleration is defined as the SRP acceleration acting on a solar sail that is oriented perpendicular to the Sun-line at 1 AU, where $F_{\text{SRP}} = F_c$, the characteristic SRP force. For model ηPR, one gets

$$a_c = \frac{F_c}{m} = 2\eta \frac{S_0}{c}\frac{A}{m} \tag{12}$$

The SRP force may then be written as

$$\mathbf{F}_{\text{SRP}} = m a_c \left(\frac{1\,\text{AU}}{r}\right)^2 \cos^2\beta\,\mathbf{n} \tag{13}$$

For model NPR, one gets

$$a_c = \frac{F_c}{m} = (G+K)\frac{S_0}{c}\frac{A}{m} \tag{14}$$

The SRP force may then be written as

$$\mathbf{F}_{\text{SRP}} = ma_c\left(\frac{1\,\text{AU}}{r}\right)^2 \frac{2Q(\beta)}{G+K}\,\mathbf{f} = ma_c\left(\frac{1\,\text{AU}}{r}\right)^2 Q'(\beta)\,\mathbf{f} \tag{15}$$

Comparing Eqs. (12) and (14), one can see that in order to get the same characteristic acceleration for model ηPR and model NPR, one has to set $\eta = (G+K)/2$ ($\doteq 0.908$ for the optical coefficients given in Table 2).

Lightness Number

The lightness number is defined as the ratio of the SRP acceleration acting on a solar sail that is oriented perpendicular to the Sun-line, and the gravitational acceleration of the Sun, $a_{\text{G}}(r) = \mu/r^2$:

$$\lambda = \frac{a_c \cdot (1\,\text{AU}/r)^2}{\mu/r^2} = \frac{a_c \cdot 1\,\text{AU}^2}{\mu} = \frac{a_c}{a_{\text{G}}(1\,\text{AU})} \tag{16}$$

with $a_{\text{G}}(1\,\text{AU}) \doteq 5.930\,\text{mm/s}^2$ as the Sun's gravitational acceleration at Earth distance. Since both accelerations have an inverse square variation in r, the lightness of solar sailcraft is – unlike the maximum acceleration – independent of the Sun–sail distance. Using Eq. (16), the SRP force may be written as

$$\mathbf{F}_{\text{SRP}} = \lambda\frac{\mu m}{r^2}\cos^2\beta\,\mathbf{n} \tag{17}$$

for model ηPR and

$$\mathbf{F}_{\text{SRP}} = \lambda\frac{\mu m}{r^2}Q'(\beta)\,\mathbf{f} \tag{18}$$

for model NPR.

EVOLUTIONARY NEUROCONTROL

Here, only a summary of evolutionary neurocontrol (ENC) can be given. The reader who is interested in details of this novel low-thrust trajectory optimization method is referred to Refs. [7, 8, 9].

It can be shown that the problem of searching an optimal spacecraft trajectory $\mathbf{x}^\star_{\text{SC}}[t] = (\mathbf{r}^\star_{\text{SC}}, \dot{\mathbf{r}}^\star_{\text{SC}})[t]$ is equivalent to the problem of searching an optimal spacecraft control function $\mathbf{u}^\star[t]$. Usually, optimal control methods that are based on the calculus of variations are employed to solve this kind of problems. Within this paper, spacecraft trajectory optimization has been attacked from a perspective different to that of optimal control: the perspective of artificial intelligence and machine learning. Within this context, a trajectory can be regarded as the result of a **spacecraft steering strategy** S that maps the problem relevant variables (e.g. the spacecraft state $\mathbf{x}_{\text{SC}}$ and the target body state $\mathbf{x}_{\text{T}}$) onto the spacecraft control vector, $\mathsf{S} : \{\mathbf{x}_{\text{SC}}, \mathbf{x}_{\text{T}}\} \subset \mathbb{R}^{12} \mapsto \{\mathbf{u}\} \subset \mathbb{R}^2$. This way, the problem of searching the optimal spacecraft trajectory is equivalent to the problem of searching (or "learning") the optimal spacecraft steering strategy $\mathsf{S}^\star$. An artificial neural network (ANN) may be used as a so-called **neurocontroller** (NC) to implement such spacecraft steering strategies. It can be regarded as a parameterized function $\mathsf{N}_{\boldsymbol{\pi}}$ (the network function) that is – for a given network topology – completely defined by the internal parameter vector $\boldsymbol{\pi} \in \mathbb{R}^{n_\pi}$ of the network. Therefore, each $\boldsymbol{\pi}$ defines a steering strategy $\mathsf{S}_{\boldsymbol{\pi}}$. The problem of searching the optimal spacecraft trajectory is thus equivalent to the problem of searching the optimal parameter vector $\boldsymbol{\pi}^\star$ for a given neurocontroller. Evolutionary algorithms (EAs) that work on a population of strings

can be used for finding the optimal network parameters, since the NC parameter vector $\boldsymbol{\pi}$ can be mapped onto a string $\boldsymbol{\xi}$ (also called chromosome or individual). The trajectory optimization problem is solved, when the optimal chromosome $\boldsymbol{\xi}^\star$ is found. Figure 5 sketches the subsequent transformations of the optimal chromosome into the optimal trajectory.

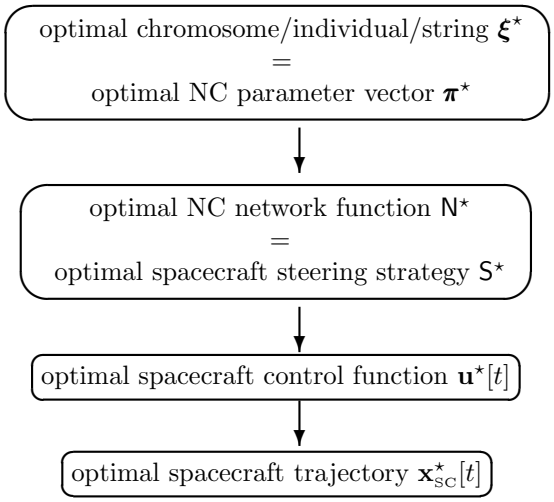

Figure 5 From the optimal chromosome to the optimal trajectory

A neurocontroller that employs an evolutionary algorithm for "learning" (or "breeding") the optimal control strategy might be called **evolutionary neurocontroller**.

SIMULATION MODEL

Besides the gravitational forces of *all* celestial bodies and the SRP force, many "disturbing" forces – as caused, e.g., by the solar wind and the aberration of solar radiation (Poynting–Robertson effect) – are influencing the motion of solar sailcraft. Ideally, all these forces have to be considered for a thorough mission analysis. However, for mission feasibility analysis, as done within this paper, only "preliminary" trajectory analysis needs to be done, which allows some simplifications:

1. Solar sailcraft is moving under the sole influence of solar gravitation and radiation. The Sun is a point mass and a point light source. All disturbing forces that are small in magnitude – compared to gravitation and solar radiation pressure – are neglected. Also ignored are the gravitational and radiative forces of other celestial bodies (including the launch and the target body).
2. The solar sailcraft's attitude can be changed instantaneously.
3. The sail film does not degrade over time.

EQUATIONS OF MOTION

Within this section, the equations of heliocentric translational motion within the given simulation model are derived for perfectly and non-perfectly reflecting solar sailcraft. Ignoring second order effects, the acceleration of solar sailcraft is simply obtained by adding the Sun's gravitational acceleration and the SRP acceleration:

$$\ddot{\mathbf{r}} = \mathbf{a}_{\mathrm{G}} + \mathbf{a}_{\mathrm{SRP}} \tag{19}$$

Resolving this equation along the unit vectors of the ecliptic reference frame $\mathcal{E} = (\mathbf{e}_r, \mathbf{e}_\varphi, \mathbf{e}_\theta)$ (Figure 6.1) will then give three 2nd order differential equations for $\ddot{r}$, $\ddot{\varphi}$, and $\ddot{\theta}$ respectively.

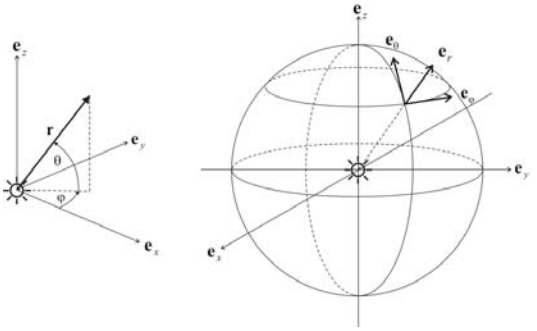

6.1: Ecliptic reference frame $\mathcal{E}$

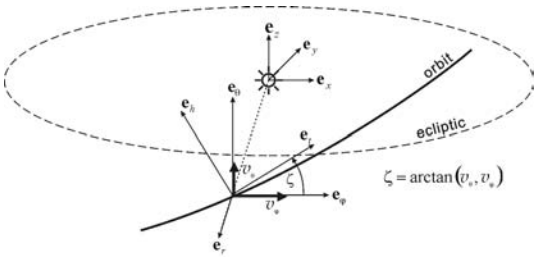

6.2: Orbit reference frame $\mathcal{O}$

Perfect Reflection (models IR and ηPR)

Using Eq. (17), one gets for the models IR and ηPR

$$\ddot{\mathbf{r}} = \lambda \frac{\mu}{r^2} \cos^2\beta\, \mathbf{n} - \frac{\mu}{r^2}\mathbf{e}_r \tag{20}$$

Resolving $\mathbf{n}$ along the unit vectors of the orbit reference frame $\mathcal{O} = (\mathbf{e}_r, \mathbf{e}_t, \mathbf{e}_h)$ (Figure 6.2), one obtains

$$\mathbf{n} = \cos\beta\mathbf{e}_r + \cos\alpha\sin\beta\mathbf{e}_t + \sin\alpha\sin\beta\mathbf{e}_h \tag{21}$$

and after transformation into the $\mathcal{E}$-frame

$$\mathbf{n} = \cos\beta\mathbf{e}_r + \cos(\alpha+\zeta)\sin\beta\mathbf{e}_\varphi + \sin(\alpha+\zeta)\sin\beta\mathbf{e}_\theta \tag{22}$$

By introducing three dimensionless control functions u_1' to u_3', depending only on the two control variables α and β, and on the local $\mathcal{E}$-$\mathcal{O}$-rotation angle ζ

$$u_1'(\beta) = \cos^3\beta \tag{23a}$$
$$u_2'(\alpha+\zeta,\beta) = \cos(\alpha+\zeta)\sin\beta\cos^2\beta \tag{23b}$$
$$u_3'(\alpha+\zeta,\beta) = \sin(\alpha+\zeta)\sin\beta\cos^2\beta \tag{23c}$$

and using Eq. (22), one may write the acceleration of the solar sailcraft in $\mathcal{E}$-frame components as:

$$\ddot{\mathbf{r}} = (\lambda\frac{\mu}{r^2}u_1' - \frac{\mu}{r^2})\mathbf{e}_r + \lambda\frac{\mu}{r^2}u_2'\mathbf{e}_\varphi + \lambda\frac{\mu}{r^2}u_3'\mathbf{e}_\theta \tag{24}$$

Expressing $\ddot{\mathbf{r}}$ in spherical coordinates, one gets – after some rearrangement – three component equations:

$$\ddot{r} = r\dot{\theta}^2 + r\dot{\varphi}^2\cos^2\theta - \frac{\mu}{r^2} + \lambda\frac{\mu}{r^2}u_1' \tag{25a}$$
$$\ddot{\varphi} = -2\frac{\dot{r}\dot{\varphi}}{r} + 2\dot{\varphi}\dot{\theta}\tan\theta + \lambda\frac{\mu}{r^2}\frac{u_2'}{r\cos\theta} \tag{25b}$$
$$\ddot{\theta} = -2\frac{\dot{r}\dot{\theta}}{r} - \dot{\varphi}^2\sin\theta\cos\theta + \lambda\frac{\mu}{r^2}\frac{u_3'}{r} \tag{25c}$$

Non-Perfect Reflection (model NPR)

Using Eq. (18), one gets for model NPR

$$\ddot{\mathbf{r}} = \lambda \frac{\mu}{r^2} Q'(\beta)\, \mathbf{f} - \frac{\mu}{r^2} \mathbf{e}_r \tag{26}$$

Resolving $\mathbf{f}$ along the $\mathcal{O}$-frame unit vectors, one obtains

$$\mathbf{f} = \cos\delta \mathbf{e}_r + \cos\gamma \sin\delta \mathbf{e}_t + \sin\gamma \sin\delta \mathbf{e}_h \tag{27}$$

and after transformation into the $\mathcal{E}$-frame

$$\mathbf{f} = \cos\delta \mathbf{e}_r + \cos(\gamma+\zeta) \sin\delta \mathbf{e}_\varphi + \sin(\gamma+\zeta) \sin\delta \mathbf{e}_\theta \tag{28}$$

where $\gamma = \alpha$ and $\delta = \beta - \arctan\left(\frac{H \sin\beta}{G\cos\beta + K}\right)$. By introducing three dimensionless control functions u'_1 to u'_3, depending only on the two control variables α and β, the local $\mathcal{E}$-$\mathcal{O}$-rotation angle ζ, and the optical characteristics of the sail film

$$u'_1(\beta) = Q'(\beta)\cos\delta(\beta) \tag{29a}$$
$$u'_2(\alpha+\zeta,\beta) = Q'(\beta)\cos(\alpha+\zeta)\sin\delta(\beta) \tag{29b}$$
$$u'_3(\alpha+\zeta,\beta) = Q'(\beta)\sin(\alpha+\zeta)\sin\delta(\beta) \tag{29c}$$

one gets again Eq. (24) and thus again Eqs. (25) but with different control functions.

MINIMAL TRANSFER TIMES FOR PERFECTLY REFLECTING SOLAR SAILCRAFT (MODELS IR AND ηPR)

Using evolutionary neurocontrol (ENC) for solar sailcraft trajectory optimization, minimal transfer times to various solar system bodies (and for an exemplary 10° inclination change at 1 AU for a circular initial and target orbit) have been calculated. Sauer gives in Ref. [4] minimal transfer times to Mercury, Venus, and Mars for perfectly reflecting high-performance sailcraft with $0.5\,\mathrm{mm/s^2} \lesssim a_c \lesssim 2.5\,\mathrm{mm/s^2}$ (Figure 6).

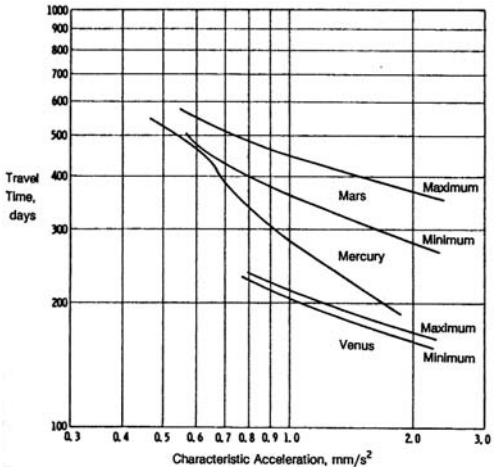

Figure 6 Upper and lower bound for minimal transfer times to Mercury, Venus, and Mars that are given by Sauer, Ref. [4] (only lower bound for Mercury, diagram taken from Wright, Ref. [5])

To verify the transfer times given by SAUER and to extend them to solar sailcraft of moderate performance ($a_c \lesssim 0.5\,\mathrm{mm/s^2}$) and extremely high performance ($a_c \gtrsim 2.5\,\mathrm{mm/s^2}$), minimal orbit transfer times to various targets have been calculated for characteristic accelerations in the range $0.1\,\mathrm{mm/s^2} \leq a_c \leq 10.0\,\mathrm{mm/s^2}$. The results are presented in Figure 7.‡

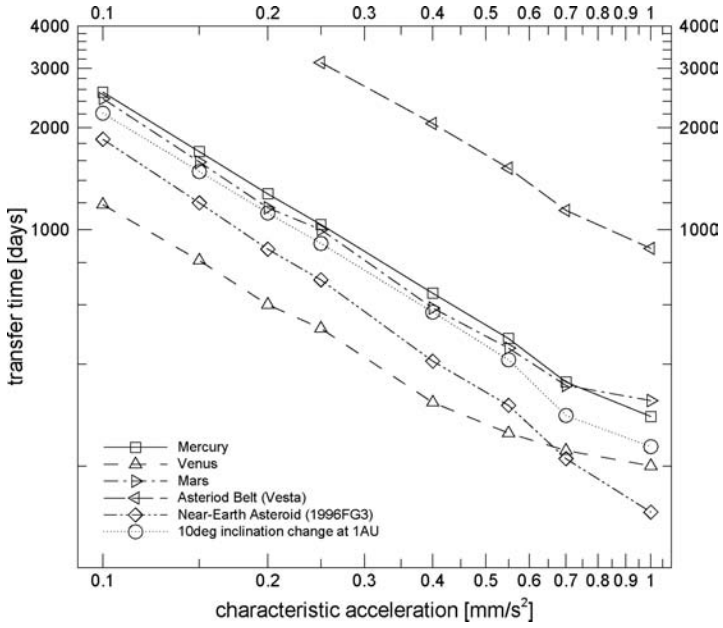

7.1: $0.1\,\mathrm{mm/s^2} \leq a_c \leq 1.0\,\mathrm{mm/s^2}$

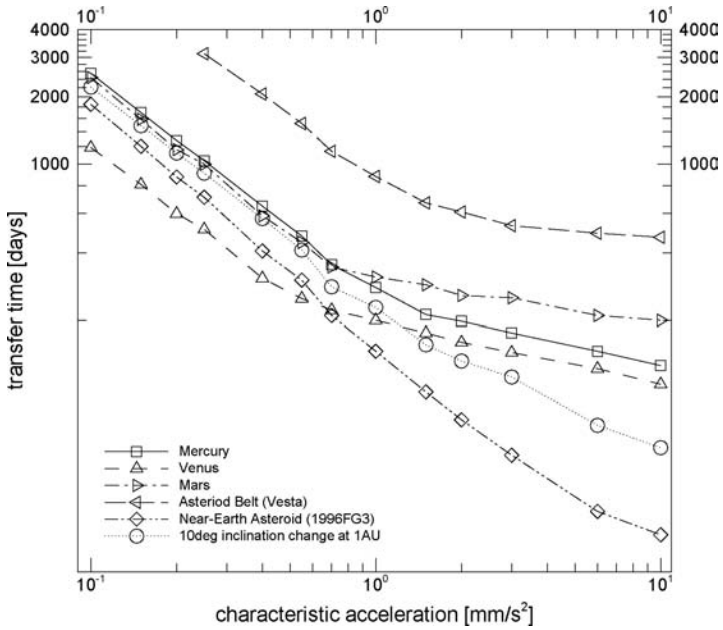

7.2: $0.1\,\mathrm{mm/s^2} \leq a_c \leq 10.0\,\mathrm{mm/s^2}$

Figure 7 Minimum orbit transfer times for perfectly reflecting solar sailcraft

‡ Note that the solution of the orbit transfer problem yields the absolute minimum for the transfer time, independent of the constellation of the initial and the target body. The optimal launch constellation for the rendezvous problem can then be deduced from the optimal solution of the orbit transfer problem.

For $0.5\,\mathrm{mm/s^2} \lesssim a_c \lesssim 2.5\,\mathrm{mm/s^2}$, they are consistent with the minimum curves in Figure 6 (see Figure 7.2). The ENC-results, however, also reveal two performance-regimes. For moderate-performance sailcraft ($a_c \lesssim 0.5\,\mathrm{mm/s^2}$) as well as for high-performance sailcraft ($a_c \gtrsim 1.0\,\mathrm{mm/s^2}$), the minimum transfer times $T_{\min}$ can be approximated with very simple functions of the form

$$\frac{T_{\min}}{1\,\mathrm{day}} = \frac{c_1}{(\frac{a_c}{1\,\mathrm{mm/s^2}})^{c_2}} \tag{30}$$

The values for c_1 and c_2 depend obviously on the target body. It can be speculated that they are a function of the initial and the target body's orbital elements (quod esset demonstrandum). For example, the approximation function

$$\frac{T_{\min,\mathrm{Mercury}}}{1\,\mathrm{day}} = \frac{255}{\frac{a_c}{1\,\mathrm{mm/s^2}}}$$

gives for $0.1\,\mathrm{mm/s^2} \leq a_c \leq 0.75\,\mathrm{mm/s^2}$ a maximum error of 4.2% for the Earth-Mercury transfer. For the Earth-1996FG$_3$ transfer, the approximation function

$$\frac{T_{\min,1996\mathrm{FG}_3}}{1\,\mathrm{day}} = \frac{146}{(\frac{a_c}{1\,\mathrm{mm/s^2}})^{1.127}}$$

gives for $0.1\,\mathrm{mm/s^2} \leq a_c \leq 1.0\,\mathrm{mm/s^2}$ a maximum error of 5.5%. Within the high-performance regime, the flight time gain due to a better sail performance is smaller. Between the two regimes, the curves bend sharply (Figure 7.2). Since the optimal trajectories for solar sailcraft to spiral inwards or outwards are logarithmic spirals, the reduced flight-time gain in the high-performance regime is more pronounced for near-circular target orbits, since they require a final "circularization" of the spiral. Where such a circularization is not required, the bending of the curves is less pronounced (1996FG$_3$, and for the 10° inclination change, for which the optimal transfer trajectory is not a logarithmic spiral).

MINIMAL TRANSFER TIMES FOR NON-PERFECTLY REFLECTING SOLAR SAILCRAFT (MODEL NPR)

Solar sailcraft trajectory/mission analyses usually employ model IR/ηPR. The only known calculations for model NPR have been done in Ref. [13], where a simple Earth-Venus-transfer and a simple Earth-Mars-transfer were calculated using a local trajectory optimization method (direct collocation method).

Within this section, the minimal orbit transfer times for solar sailcraft are calculated using model NPR. The results are compared to the transfer times that have been obtained above for perfectly reflecting solar sailcraft. For all calculations, the *size* of the SRP force bubbles was the same ($a_{c,\mathsf{NPR}} = a_{c,\mathsf{IR}/\eta\mathsf{PR}}$). Figure 8 shows a comparison of the minimal transfer times to various solar system bodies for perfectly and for non-perfectly reflecting solar sailcraft.

As the results show, there is a considerable increase of about $5 - 15\%$ in minimal orbit transfer time, if model NPR is used, being larger for trajectories that require large sail cone angles, where the difference between the perfect and the non-perfect bubble is larger (see Figure 5.2). It might be argued that trajectory optimization for non-perfectly reflecting solar sails is more difficult for the ENC method, so that it fails to find globally optimal solutions. Although a part of the differences might be attributed to this cause, such an explanation is unlikely to explain the entire differences. The results are in accordance with the result in Ref. [13], where an increase of 7.8% in transfer time had been obtained for a simple Earth-Mars-transfer ($a_c \doteq 1.5\,\mathrm{mm/s^2}$). For a simple Earth-Venus-transfer, an increase of even 24% in transfer time (306 days for $a_c \doteq 0.55\,\mathrm{mm/s^2}$) had been obtained in Ref. [13], which suggests, however, that the trajectory is far from the global optimum (ENC optimization yields a minimum transfer time of 268 days for exactly the same problem).

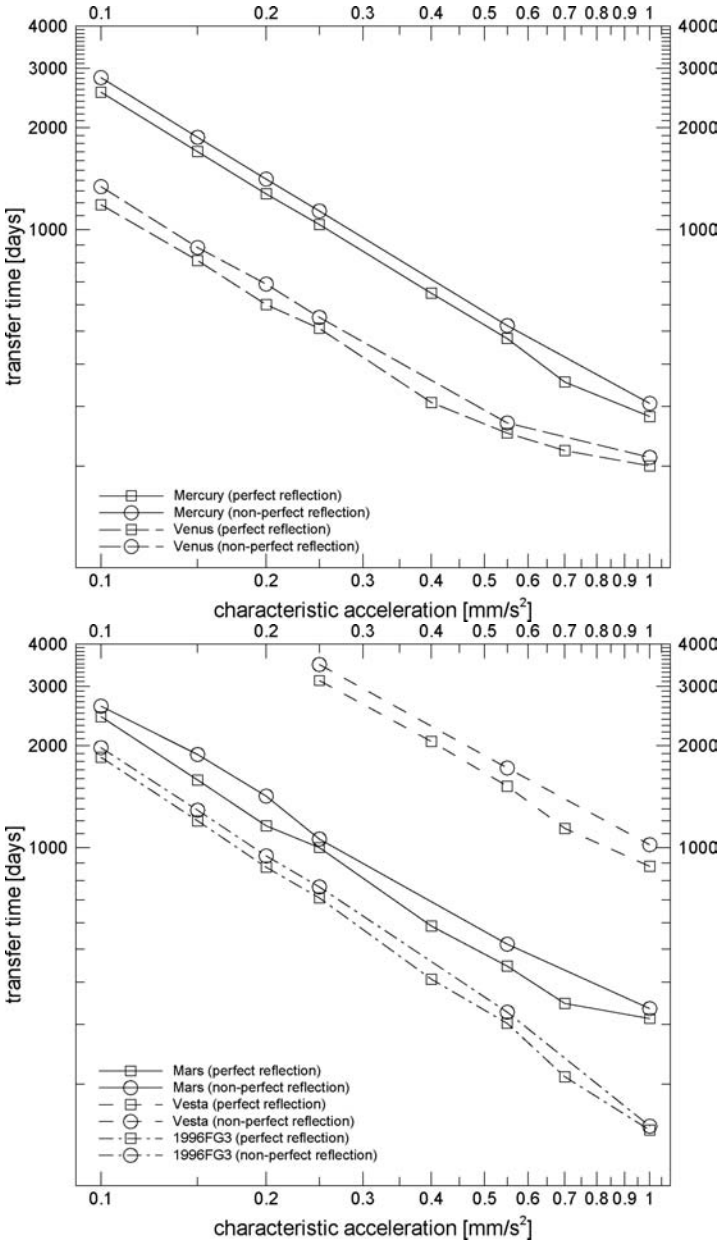

Figure 8 Comparison of minimum orbit transfer times for perfectly and non-perfectly reflecting solar sailcraft

The results demonstrate that for a thorough mission analysis the non-perfect reflectivity of the solar sail must be considered through an appropriate SRP force model. The simplification that the non-ideal reflectivity of the sail can be taken into account by using an overall efficiency factor η, should only be made for *very* preliminary mission feasibility analyses.

SUMMARY AND CONCLUSIONS

Using evolutionary neurocontrol as a global trajectory optimization method, minimal transfer times for rendezvous missions to inner solar system bodies have been calculated for perfectly and for non-perfectly reflecting solar sailcraft. Thereby, the currently available data was extended to moderate-performance sailcraft and in the case of perfect reflection also to very-high performance sailcraft. For perfectly reflecting solar sailcraft, two performance-regimes have been found – one for moderate-performance sailcraft and one for high-performance sailcraft – in which the minimum transfer times can be approximated with very simple functions. Within the high-performance regime, the flight time gain due to better sail performances is smaller, especially for near-circular target orbits, where a circularization of the logarithmic transfer spiral is required. Trajectory optimization using evolutionary neurocontrol revealed that for non-perfectly reflecting solar sailcraft there is a considerable increase of about $5 - 15\%$ in the minimal transfer times that must be considered for a thorough mission analysis. The simplification that the non-ideal reflectivity of a real solar sail can be taken into account by using an overall sail efficiency factor should therefore only be made for very preliminary mission analyses.

References

[1] M. Leipold. *Solar Sail Mission Design*. Doctoral thesis, Lehrstuhl für Flugmechanik und Flugregelung; Technische Universität München, 1999. DLR-FB-2000-22.

[2] M. Leipold, E. Pfeiffer, P. Groepper, M. Eiden, W. Seboldt, L. Herbeck, and W. Unkenbold. Solar sail technology for advanced space science missions. Toulouse, France, 2001. 52nd International Astronautical Congress. IAF-01-S.6.10.

[3] M. Leipold, W. Seboldt, S. Lingner, E. Borg, A. Herrmann, A. Pabsch, O. Wagner, and J. Brückner. Mercury sun-synchronous polar orbiter with a solar sail. *Acta Astronautica*, 39(1-4):143–151, 1996.

[4] C. G. Sauer. Optimum solar-sail interplanetary trajectories. San Diego, USA, August 1976. AIAA/AAS Astrodynamics Conference. AIAA 76-792.

[5] J. L. Wright. *Space Sailing*. Gordon and Breach Science Publishers, Philadelphia, 1992.

[6] R. H. Battin. *An Introduction to the Mathematics and Methods of Astrodynamics*. AIAA Education Series. American Institute of Aeronautics and Astronautics, Reston, revised edition, 1999.

[7] B. Dachwald and W. Seboldt. Optimization of interplanetary rendezvous trajectories for solar sailcraft using a neurocontroller. Monterey, USA, August 2002. AIAA/AAS Astrodynamics Specialist Conference. AIAA-2002-4989.

[8] B. Dachwald. Optimization of interplanetary solar sailcraft trajectories using evolutionary neurocontrol. *Journal of Guidance, Control, and Dynamics*. accepted for publication.

[9] B. Dachwald. *Low-Thrust Trajectory Optimization and Interplanetary Mission Analysis Using Evolutionary Neurocontrol*. Doctoral thesis, Universität der Bundeswehr München; Fakultät für Luft- und Raumfahrttechnik; Institut für Raumfahrttechnik. submitted.

[10] C. R. McInnes. *Solar Sailing. Technology, Dynamics and Mission Applications*. Springer–Praxis Series in Space Science and Technology. Springer–Praxis, Berlin, Heidelberg, New York, Chicester, 1999.

[11] D. M. Murphy, T. W. Murphy, and P. A. Gierow. Scalable solar sail subsystem design considerations. Denver, USA, April 2002. AIAA 43rd Structures, Structural Dynamics, and Materials Conference. AIAA-2002-1703.

[12] R. Sachs. Interplanetare Transferbahnen für Sonnensegler-Missionen. Diploma thesis, DLR, Forschungsbereich Flugmechanik / Flugführung, Hauptabteilung Systemanalyse Raumfahrt, October 1994. (in German).

[13] T. Cichan and R. Melton. Optimal trajectories for non-ideal solar sails. Quebec, Canada, August 2001. AAS/AIAA Astrodynamics Specialist Conference. AAS 01-471.